



Comparison of high- and low-state X-ray spectra in the type 1.5 quasi-stellar object 2MASS 0918+2117

Citation

Pounds, K. A., and B. J. Wilkes. 2007. "Comparison of High- and Low-State X-Ray Spectra in the Type 1.5 Quasi-Stellar Object 2MASS 0918+2117." *Monthly Notices of the Royal Astronomical Society* 380 (4) (October 1): 1341–1347. doi:10.1111/j.1365-2966.2007.12205.x.

Published Version

doi:10.1111/j.1365-2966.2007.12205.x

Permanent link

<http://nrs.harvard.edu/urn-3:HUL.InstRepos:29921876>

Terms of Use

This article was downloaded from Harvard University's DASH repository, and is made available under the terms and conditions applicable to Other Posted Material, as set forth at <http://nrs.harvard.edu/urn-3:HUL.InstRepos:dash.current.terms-of-use#LAA>

Share Your Story

The Harvard community has made this article openly available.
Please share how this access benefits you. [Submit a story](#).

[Accessibility](#)

Comparison of high- and low-state X-ray spectra in the type 1.5 quasi-stellar object 2MASS 0918+2117

K. A. Pounds^{1*} and B. J. Wilkes²

¹*Department of Physics and Astronomy, University of Leicester, Leicester LE1 7RH*

²*Harvard-Smithsonian Center for Astrophysics, 60 Garden Street, Cambridge, MA 02138, USA*

Accepted 2007 July 6. Received 2007 June 25; in original form 2007 May 15

ABSTRACT

When observed by *XMM-Newton* in 2003, the type 1.5 quasi-stellar object 2MASS 0918+2117 was found to be in a low state, with an X-ray flux approximately four to five times fainter than during an earlier *Chandra* observation. The 2–6 keV spectrum was unusually hard (photon index $\Gamma \sim 1.25$), with evidence for a reflection-dominated continuum, while a soft excess visible below ~ 1 keV prevented confirmation of the anticipated low energy absorber. In a second *XMM-Newton* observation in 2005, the X-ray flux is found to have recovered, with a 2–10 keV continuum spectrum now typical of a broad-line active galaxy ($\Gamma \sim 2$) and a deficit of flux below ~ 1 keV indicative of continuum absorption in a column $N_{\text{H}} \sim 4 \times 10^{21} \text{ cm}^{-2}$. We find the preferred ionization state of the absorbing gas to be low, which then leaves a residual soft excess of similar spectral form and flux to that found in the 2003 *XMM-Newton* observation. Although observed at different epochs, we note that dust in the absorbing column could also explain the red nucleus and strong optical polarization of 2MASS 0918+2117.

Key words: galaxies: active – galaxies: general – galaxies: individual: 2MASS 0918+2117 – quasars: general – X-ray: galaxies.

1 INTRODUCTION

The Two-Micron All-Sky Survey (2MASS) has revealed many highly reddened active galaxies [active galactic nuclei (AGN)] whose number density rivals that of optically selected AGN. Spectroscopic follow-up of red candidates showed ~ 75 per cent to be previously unidentified emission-line AGN, with ~ 80 per cent of those showing the broad optical emission lines of type 1 Seyfert galaxies and quasi-stellar objects (QSOs) (Cutri et al. 2001). These objects often have unusually high optical polarization levels, with ~ 10 per cent showing $P > 3$ per cent indicating a significant contribution from scattered light (Smith et al. 2002) and suggesting substantial obscuration towards the nuclear energy source. *Chandra* observations of a sample of 2MASS AGN found them to be X-ray weak with generally flat (hard) spectra (Wilkes et al. 2002).

While cold absorption is an expected signature in reddened AGN, *XMM-Newton* follow-up observations of a subset of five 2MASS AGN (Wilkes et al. 2005, hereafter W05) showed a mixed picture. The longer *XMM-Newton* exposures confirmed a substantial column of cold matter ($N_{\text{H}} \sim 10^{22} \text{ cm}^{-2}$) in two cases, both optical type 2 AGN. In two further cases, both optical type 1, low energy absorption was apparent in one, although complicated by a soft emission component (Pounds, Wilkes & Page 2005). The fifth object in the *XMM-Newton* sample, 2MASS 0918+2117, was potentially the

most interesting, being optically classified as an intermediate type 1.5 QSO at a redshift of $z = 0.149$ (Cutri et al. 2003). However, the data on 2MASS 0918+2117 were of low quality due to the source being unexpectedly faint.

2MASS 0918+2117 was selected for the initial *Chandra* sample due to its unusually ‘red’ nucleus ($J - K_s \sim 2.23$) and high optical polarization of ~ 6.4 per cent (Smith et al. 2002, 2003). Given that evidence of strong nuclear obscuration, the *Chandra* detection of a ‘normal’ type 1 X-ray spectrum ($\Gamma \sim 1.9$), with only marginal evidence of a cold absorber, was a surprise (W05). That issue remained unclear after the first *XMM-Newton* observation of 2MASS 0918+2117 in 2003, which found a much harder overall spectrum ($\Gamma \sim 1.25$) than seen by *Chandra*, while the X-ray flux was a factor of ~ 4 –5 fainter.

Extrapolating the hard (2–10 keV) power law down to 0.3 keV (fig. 1 in W05) revealed a clear soft excess, the presence of which potentially could have ‘hidden’ the effects of low energy absorption in the *Chandra* spectrum, while an excess of counts in the highest energy channels was suggestive of reflection. Including a strong cold reflection component in the model, W05 found the power-law index increased by ~ 0.3 . Although not required by the data, inclusion of an absorbing column at the 1σ upper bound indicated by *Chandra* further increased the intrinsic continuum slope closer to the ‘normal’ $\Gamma \sim 1.8$ –2 range for unobscured AGN (Nandra & Pounds 1994).

As the soft excess remained, a broad Gaussian emission ‘line’ was included in the final 0.3–10 keV spectral model. The parameters of the best-fitting model were an underlying power-law index $\Gamma =$

*E-mail: kap@le.ac.uk

1.65 ± 0.33 , with cold reflection $R = 6 \pm 3$, and a Gaussian emission line at 0.44 ± 0.13 keV, with line width $\sigma = 75$ eV and flux $\sim 4 \times 10^{-5}$ photon $\text{cm}^{-2} \text{s}^{-1}$.

In summary, the first *XMM-Newton* observation of 2MASS 0918+2117 found the source in a low flux state, with a hard power-law continuum probably dominated by a strong reflection component (W05). The hard continuum, in turn, allowed the soft excess to stand out, but evidence of the X-ray absorption that might be expected for such a highly reddened AGN remained unclear.

Here, we report the outcome of a second, longer *XMM-Newton* observation of 2MASS 0918+2117, finding the X-ray flux to be now a factor of ~ 2 brighter than when observed by *Chandra*.

2 OBSERVATION AND DATA REDUCTION

The new *XMM-Newton* observation of 2MASS 0918+2117 took place on 2005 November 15/16. The EPIC pn (Strüder et al. 2001) and MOS1 and MOS2 (Turner et al. 2001) cameras obtained CCD-resolution spectra over the energy band ~ 0.2 –10 keV. Each EPIC camera was set in large window mode, with the thin filter (as in the first observation). Unfortunately, the source was too weak to get useful high-resolution spectra from the grating spectrometers, while the only active Optical Monitor (OM) channel (UVW1) yielded a magnitude of 19.3, identical with that in the 2003 observation. We conclude from the latter that the AGN is probably highly obscured in this *UV* band.

EPIC X-ray data were screened with the *XMM* SAS v7.0 software and events corresponding to patterns 0–4 (single and double pixel events) selected for the pn data and patterns 0–12 for MOS. A low energy cut of 300 eV was applied to all X-ray data and known hot or bad pixels were removed. Source counts were obtained from a circular region of 45 arcsec radius centred on the target source, with the background being taken from a similar region offset from, but close to, the source. Resulting exposures were 19570 s (pn) and 43149 s (combined MOS).

The X-ray flux from 2MASS 0918+2117 was found to have increased by a factor of ~ 10 from the earlier *XMM-Newton* observation. Together with the longer exposures, the brighter X-ray source meant the number of counts was greatly increased, to 11756 in the pn camera (288 in 2003) and 8034 (241) in the MOS. As the X-ray light curve showed only small variations (but see later) the integrated pn and MOS spectra were used for spectral fitting, each data set being grouped to a minimum of 20 counts per bin to facilitate the use of the χ^2 minimization technique. Spectral fitting was based on the XSPEC package (Arnaud 1996), with all spectral fits including absorption due to the line-of-sight Galactic column of $N_{\text{H}} = 4.1 \times 10^{20} \text{ cm}^{-2}$. Errors are quoted at the 90 per cent confidence level ($\Delta\chi^2 = 2.7$ for one interesting parameter).

3 SPECTRAL FITTING

The fluxed spectra from the 2005 observation of 2MASS 0918+2117 (Fig. 1) show a spectral slope typical of a type 1 AGN (approximately flat in this plot) over the 2–6 keV band. Below ~ 2 keV is a clear signature of continuum absorption, while in the highest energy channels of both pn and MOS spectra there appears to be additional absorption structure.

Initial spectral modelling proceeded in three steps. First, a power-law fit to the 2–6 keV data, a spectral region expected to be least affected by absorption, was found to be statistically acceptable ($\chi^2 = 220$ for 201 degrees of freedom) with $\Gamma = 1.78 \pm 0.07$ (pn) and $\Gamma = 1.77 \pm 0.07$ (MOS).

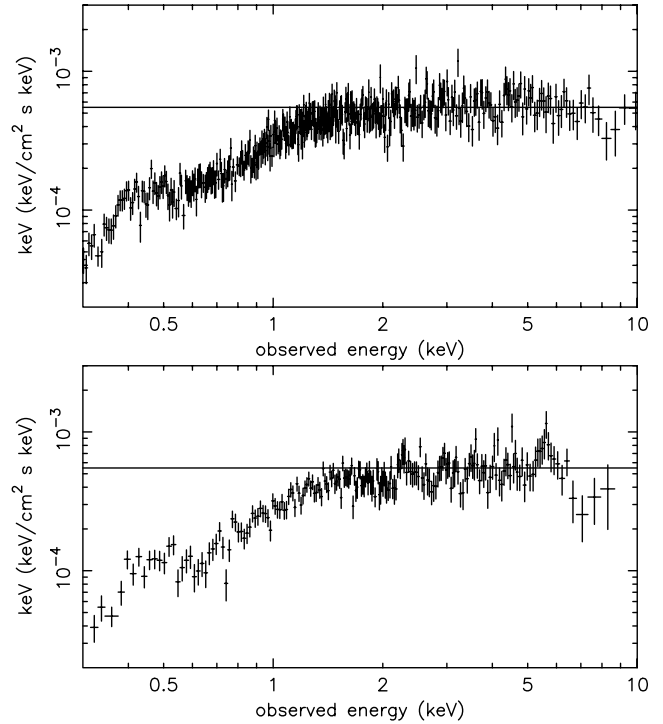


Figure 1. Fluxed pn (upper panel) and MOS spectra (lower panel) from the 2005 observation of 2MASS 0918+2117. The typical spectral slope of a type 1 AGN ($\Gamma = 2$ is flat in this plot) can be seen over the 2–6 keV band, together with clear evidence for low energy absorption.

Extending the 2–6 keV power-law fits down to 0.3 keV (Fig. 2a) reveals a flux deficit below ~ 2 keV. To model this in XSPEC, we added ABSOR1 to the power-law continuum, with free parameters of column density and ionization parameter $\xi (= L/nr^2)$, where n is the particle density at a distance of r from a source of ionizing luminosity L .

This gave a reasonably good fit (χ^2 of 605/582), with an absorbing column of $N_{\text{H}} \sim 3.7 \times 10^{21} \text{ cm}^{-2}$ of weakly ionized gas ($\xi \sim 0.11 \text{ erg cm s}^{-1}$). Interestingly, an inspection of the data of model ratio in this fit (Fig. 2b) shows some residual spectral structure, with a hint of emission features near ~ 0.4 and ~ 0.6 keV, similar to those seen in the 2003 observation. To quantify those features, we then added Gaussian lines to the XSPEC model, finding two narrow ($\sigma = 35$ eV) ‘emission lines’, at ~ 0.40 keV (0.46 keV in the AGN rest frame) and ~ 0.60 keV (0.69 keV) to give an excellent overall fit, with χ^2 of 574/578 (Fig. 2c). If the soft emission arises from a photoionized/photoexcited gas, then the Gaussian structures could be identified with resonance emission from He- and H-like ions of N and O. The parameters of the best-fitting absorbed power-law plus Gaussian line model are summarized in Table 1.

Based on the above broad-band fit, the X-ray luminosity of 2MASS 0918+2117 can be computed, finding over the full 0.3–10 keV band an observed luminosity of $1.2 \times 10^{44} \text{ erg s}^{-1}$, a factor of ~ 8.5 greater than that observed in the 2003 observation. In the soft X-ray band (0.3–1 keV), the luminosity was $1.4 \times 10^{43} \text{ erg s}^{-1}$, with $\sim 2.7 \times 10^{42} \text{ erg s}^{-1}$ in the soft emission component.

The absorption-corrected 2–6 keV luminosity of $8.5 \times 10^{43} \text{ erg s}^{-1}$ allows an estimate to be made of the bolometric luminosity of 2MASS 0918+2117, using the scaling established for a wide range of AGN (Marconi et al. 2004). We find $L_{\text{bol}} \sim 2.5 \times 10^{45} \text{ erg s}^{-1}$.

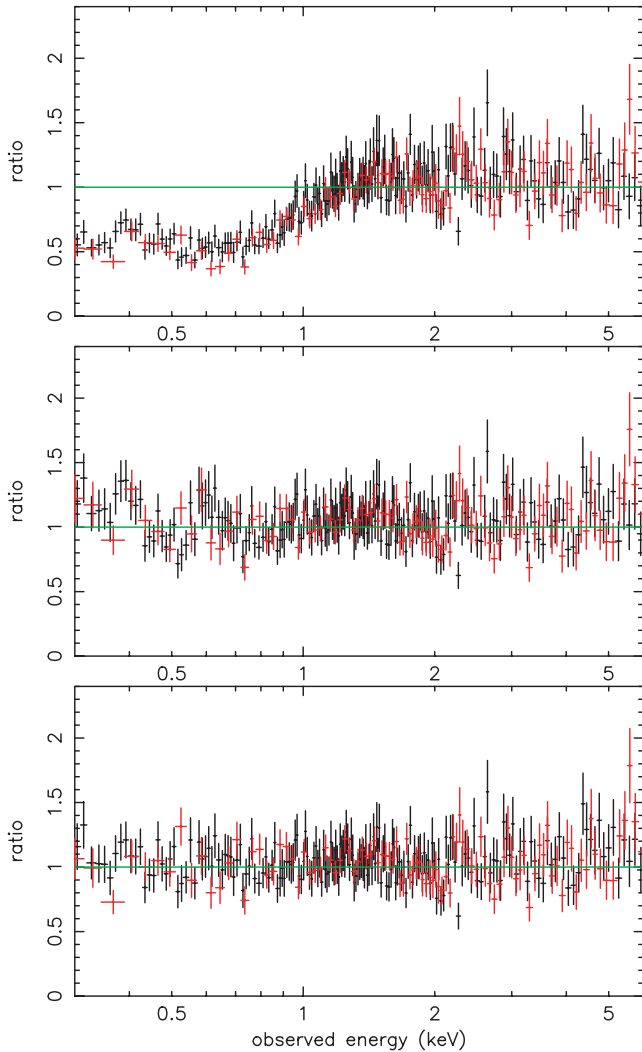


Figure 2. The pn (black) and MOS (red) data to model ratios over the 0.3–6 keV band for (a) the 2–6 keV power-law continuum, (b) power-law plus weakly ionized absorber and (c) with the further addition of Gaussian line emission, as described in the text.

4 THE NATURE OF THE SPECTRAL CHANGE BETWEEN THE LOW AND THE HIGH FLUX STATES

The spectral form observed in the low and the high flux *XMM–Newton* observations of 2MASS 0918+2117 are markedly different, with the *Chandra* spectrum sitting closer in form and flux level to the latter. The high flux *XMM–Newton* spectrum is the best defined and can be understood in terms of a typical type 1 AGN X-ray continuum attenuated at low energies by an absorbing column which – if ‘cold’ – may also explain the strong nuclear reddening of 2MASS

0918+2117. Weak residual soft X-ray features are consistent with the soft excess seen in the low flux spectrum.

Least well defined, as a result of the much lower counts, is the nature of the hard X-ray spectrum in the 2003 *XMM–Newton* observation. W05 suggested this was due to strong reflection based on an upturn in the highest energy channels. Importantly, given the optical characteristics of 2MASS 0918+2117, absorption could not be usefully constrained in that observation. Now having found a substantial cold column in the 2005 spectrum, could a much larger column have caused the hard spectral form in 2003?

The ratio of spectral data between observations at different flux levels is an established way of testing for variable multiplicative components, such as absorption. To check the above suggestion, we therefore calculated the spectral ratios of the low to the high flux observations of 2MASS 0918+2117 for both pn and MOS data. The results were similar and are reproduced for the pn data in Fig. 3. The low-to-high flux ratio is flat over the ~1–5 keV band, but increases at both low- and high-energy ends of the spectrum. Although the statistics are rather poor, limited by the low flux data points, the flat mid-section of the ratio plot *does not* have the form of variable absorption (in contrast e.g. with 1H0419–577; Pounds et al. 2004).

On the other hand, the increases in the lowest and the highest energy channels *are* consistent with the cold reflection and soft emission components suggested in the low flux modelling (W05) being less variable than the power-law continuum. A similar finding has been reported from extended studies of the bright type 1 Seyferts MCG-6-30-15 (Fabian & Vaughan 2003) and 1H 0419-577 (Pounds et al. 2004).

The above interpretation of the ratio plots, where the dominant spectral change is driven by a variable strength type 1 power law, is supported by visual examination of the data sets. This is illustrated in Fig. 4, where the pn data from both high and low flux observations are compared with a simple power-law continuum, fitted with a common power-law index ($\Gamma \sim 1.8$) over the restricted 2–5 keV band. The power law is seen to match *both* data sets quite well over an intermediate spectral band where the effects of absorption and reflection are least likely to be seen.

4.1 Absorption and emission features in the Fe K band

The fluxed spectra in Fig. 1 show evidence for absorption above ~6 keV in both pn and MOS data, while the MOS spectrum also shows a possible emission line close to the energy of neutral Fe K. When re-plotted as a ratio of data to the 2–6 keV power-law fit (Fig. 5) the pn and the MOS features appear different, particularly in the more obvious Fe K emission line and lower energy of the absorption ‘line’ in the MOS spectrum. Although the MOS sensitivity falls more steeply than the pn at high energies, in-flight data show the absolute energy calibration of the pn and the MOS cameras to agree to within a few eV in the Fe K band. However, there are well-known – and different – features in the EPIC background spectra (Strüder et al. 2001; Turner et al. 2001). To explore whether such features in the background could be contributing to the apparent high-energy

Table 1. Summary of the fit parameters for 2MASS 0918+2117 over the 0.3–10 keV band. As described in the text, the model is a power law, with weakly ionized absorption plus residual soft X-ray emission represented by Gaussian lines g1 and g2. Line energies are in the source rest frame and fluxes are in units of 10^{-5} ph cm $^{-2}$ s $^{-1}$.

Camera	Γ	N_{H} (cm $^{-2}$)	ξ (erg cm s $^{-1}$)	g1 (keV)	g1 flux	g2 (keV)	g2 flux
pn	2.12 ± 0.11	$4.0 \pm 0.3 \times 10^{21}$	0.03 ± 0.02	0.69 ± 0.02	2 ± 1.5	0.46 ± 0.02	8 ± 4
MOS	2.04 ± 0.11	$4.0 \pm 0.3 \times 10^{21}$	0.03 ± 0.02	0.69 ± 0.03	2 ± 1.5	0.46 ± 0.02	8 ± 4

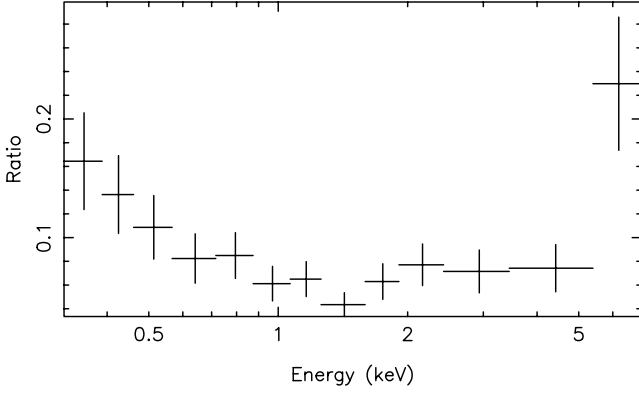


Figure 3. Ratio of low to high flux data for the pn camera, supporting the indication from spectral modelling that cold reflection and a soft emission component are less evident when 2MASS 0918+2117 is in a bright state. Importantly, the ratio plot is not consistent with the main spectral change being due to an increase in low energy absorption in the low flux state

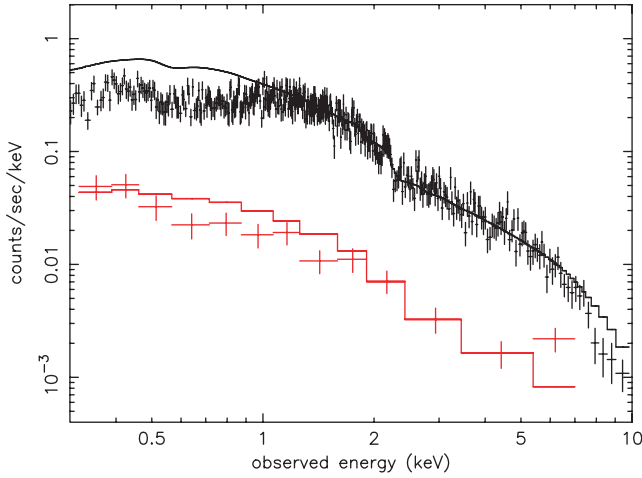


Figure 4. Comparison of data and model after fitting both 2003 (red) and 2005 (black) pn camera spectra to a common power-law index between 2 and 5 keV ($\Gamma = 1.8$).

spectral structure we show, in Fig. 6, directly comparable source and background spectra, obtained from regions of the same area on each *XMM-Newton* image.

These plots raise doubts about the background-subtracted spectra above ~ 7 keV in the MOS and above ~ 8 keV in the pn data. We therefore decided to assess spectral structure in the Fe K band by fitting the source data, without background subtraction, for the pn and the MOS cameras combined. Starting with the extrapolated 2–6 keV power-law fits, we sequentially added an emission line and two absorption edges/lines to the power-law continuum. A narrow emission line at 5.59 ± 0.07 keV (rest frame 6.42 ± 0.07 keV) was only marginally significant in the combined data set, with an equivalent width (EW) of 75 ± 50 eV and a small improvement in the fit from χ^2 of 269/228 to χ^2 of 264/226. An absorption line at 6.88 ± 0.05 keV (rest frame 7.91 ± 0.05 keV), of width $\sigma \sim 100$ eV and EW 360 ± 50 eV, produced a larger improvement, to χ^2 of 236/223. Finally, an absorption edge at 7.6 ± 0.2 keV (rest frame 8.7 ± 0.2 keV), optical depth τ of 0.3 ± 0.1 , further improved the fit to χ^2 of 228/221.

We defer further discussion of these features to Section 5.3.

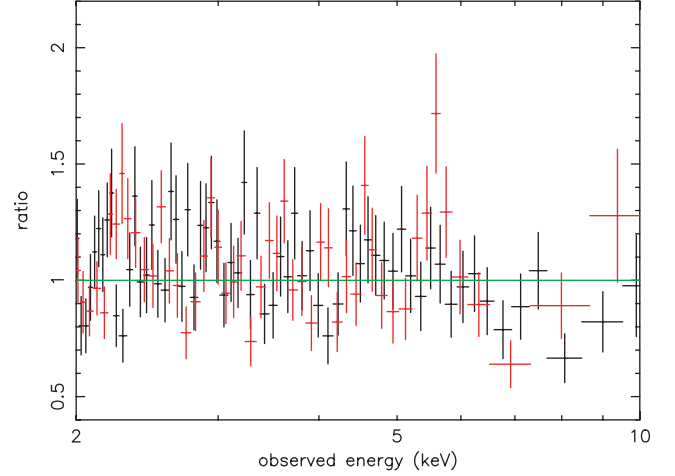


Figure 5. Ratio of source-only data to the 2–6 keV power-law fit for the 2005 observation of 2MASS 0918+2117. The pn (black) and MOS (red) source spectra show differences in apparent emission and absorption features in the Fe K band

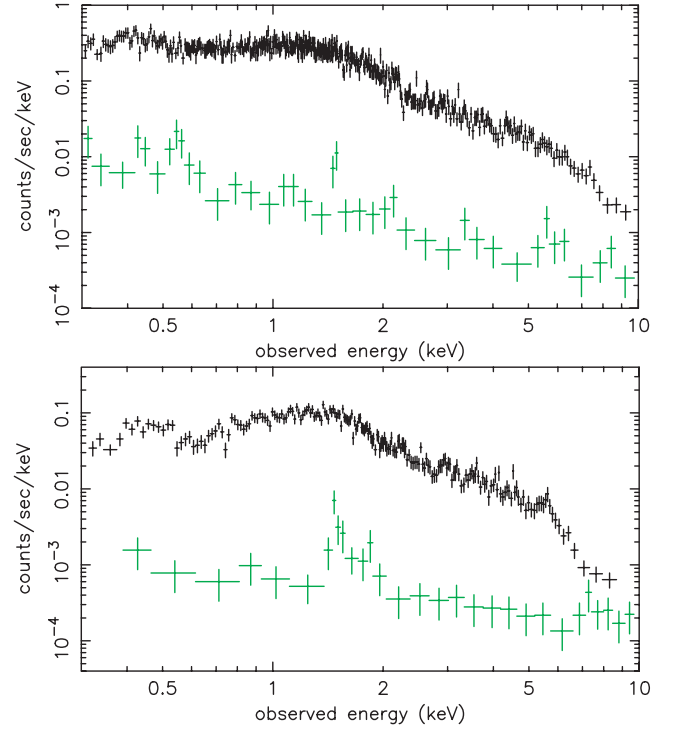


Figure 6. Source and background spectra showing the increases in background count rate near ~ 6 and ~ 8 keV (pn camera, upper panel) and ~ 7 keV (MOS camera, lower panel) which raise doubts about the apparent high energy absorption features in Figs 1 and 5.

5 DISCUSSION

5.1 Low energy absorption

The marginal detection of low energy absorption in the original *Chandra* observation of 2MASS 0918+2117 (Wilkes et al. 2002) was a surprise, given that 2MASS 0918+2117 is a highly reddened object. On the basis of the follow-up *XMM-Newton* observations it now seems that the intermediate flux level *Chandra* observation may have been confused by the presence of a soft emission component,

seen more clearly in the low flux state *XMM-Newton* observation in 2003. We now find, in the 2005 high-state spectrum, clear evidence for low energy absorption corresponding to a line-of-sight column $N_{\text{H}} \sim 4 \times 10^{21} \text{ cm}^{-2}$. With the low ionization parameter and a ‘normal’ dust to gas ratio, that absorbing column is consistent with the additional optical reddening (i.e. above that of an unobscured QSO; Barkhouse & Hall 2001) of $J - K_s \sim 0.4$ seen in 2MASS 0918+2117.

Our analysis suggests that the spectral change between the 2003 and the 2005 *XMM-Newton* observations was dominated by a change in the X-ray power-law continuum, with absorption in a column of $N_{\text{H}} \sim 4 \times 10^{21} \text{ cm}^{-2}$ of ‘cold’ or weakly ionized gas present in both cases. As noted in W05, inclusion of such absorption in modelling the 2003 *XMM-Newton* spectrum, in addition to strong cold reflection, would allow the underlying continuum to assume a ‘normal’ photon index, in the range predicted by Comptonization models (e.g. Haardt, Maraschi & Ghisellini 1997). Variability of the primary power-law continuum has been identified as the dominant component in X-ray spectral changes in several well-studied AGN (Fabian & Vaughan 2003; Pounds et al. 2004). It appears that 2MASS 0918+2117 is a further example of that situation.

While we have no direct information on the location of the absorbing gas, it is probably not very close to the central source unless in sufficiently dense clouds to avoid evaporation. However, the intermediate type 1.5 classification of 2MASS 0918+2117 suggests some absorbing matter is located at a radius comparable with the broad line region (BLR). Future observations to check for variability of the absorbing column and/or ionization parameter should clarify that issue.

5.2 Soft X-ray emission

It is interesting to speculate on the nature of the soft X-ray emission which, although obviously not well constrained in either case, is seen in both the 2003 and the 2005 observations. At face value the luminosity of the structured soft X-ray emission is higher in the 2005 observation, with $2.7 \times 10^{42} \text{ erg s}^{-1}$ in the two Gaussian components, a factor of ~ 4 greater than the similarly defined ‘soft excess’ in the 2003 observation. While the ‘soft excess’ is not determined independently of either the absorbing column or the strength and slope of the power-law continuum, light curves for 0.3–1.0 and 1–10 keV data (Fig. 7) indicate that the soft flux is less variable within the 2005 observation, suggesting a significant soft component is separate from (and more extended than) the power-law source.

To obtain a further measure of the longer term variability of the soft X-ray component, we have tried fitting the 2003 data to the 2005 spectral model (absorbed power-law plus soft excess) with the power-law slope and cold absorber fixed. The major difference was found to be in the normalization of the power law, which fell by a factor of ~ 14 . Half the remaining excess in χ^2 was removed by allowing the power-law index to change, a reduction from ~ 2.1 to ~ 1.9 perhaps corresponding to the relatively stronger reflection in the low flux spectrum. Finally, the soft X-ray emission was allowed to vary, an acceptable fit being obtained for a fall in Gaussian line flux of a factor of ~ 1.6 .

While the above estimate is model dependent, and a constant soft flux is not ruled out, it is clear that the soft X-ray emission component, significant in both *XMM-Newton* observations, is much less variable than the power-law continuum. The relative lack of variability supports an origin of the soft X-ray emission in an extended outflow, as is actually resolved in nearby type 2 AGN. That physical

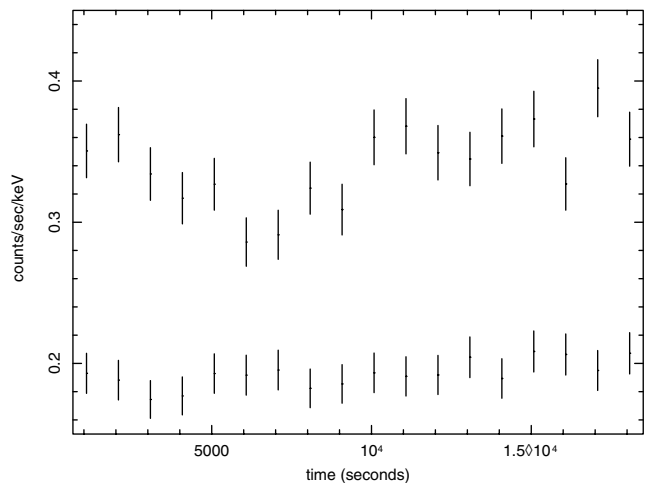


Figure 7. X-ray light curve from the 2005 observation. The upper plot for the 1–10 keV band shows evidence for variability on the time-scale of 2–3000 s which is not replicated in the soft 0.3–1 keV flux shown below.

link has been proposed in the analysis of the X-ray spectra of other type 1 AGN and a quantitative comparison made in Pounds et al. (2005). We revise this comparison here and add our new analysis for 2MASS 0918+2117.

Table 2 summarizes the results, where the 2–10 keV luminosities, corrected for absorption in our line of sight, are used as a proxy for the ionizing flux irradiating the soft X-ray emission region. The data indicate a trend where the relative strength of the soft X-ray emission in type 1 AGN is typically an order of magnitude greater than for type 2 AGN. The intermediate value for 2MASS 0918+2117 is consistent with its intermediate optical type, supporting the view that the soft X-ray emission typically arises from an ionized outflow originating at a smaller radius the BLR, possibly driven off the same cold matter seen in absorption. In that context, we note that energetically the soft X-ray emission in the 2005 observation of 2MASS 0918+2117 corresponds to only ~ 5 per cent of the power-law continuum flux removed by the cold absorber.

5.3 Evidence for absorption in highly ionized gas?

Analysing the high-energy spectrum of 2MASS 0918+2117 is unusually challenging due to the presence of apparently quite strong emission and absorption features which, however, are not consistent between the pn and the MOS data. These differences remain, although at a reduced level, when the background subtraction is removed. Finding no other explanation than limited statistics, we therefore analysed the source-only spectra for the pn and the MOS data combined.

We find a marginally significant emission line at an energy consistent with Fe K fluorescence from low ionization matter. The equivalent width is consistent with continuum reflection being much less significant (relative to the direct power law) than in the 2003 observation. At the low level detected, scattering from the cold absorber might be a candidate source.

A stronger fall in sensitivity in the Fe K band would explain why the MOS camera only detects the absorption feature observed at ~ 6.9 keV (~ 7.9 keV in the AGN rest frame). Fig. 5 suggests an absorption line, rather than an absorption edge, and indeed that choice is statistically preferred. If real, the most likely identification is with resonance line absorption in highly ionized Fe. For He-like

Table 2. The soft X-ray and 2–10 keV luminosities of 2MASS 0918+2117 from the 2005 observation, together with comparable luminosities for three type 1 AGN and for the archetypal type 2 AGN, Mkn3 and NGC 1068. The soft X-ray emission luminosities are as observed and as corrected for absorption in our Galaxy. With the 2–10 keV luminosities, corrected for intrinsic absorption, used as a proxy for the ionizing flux irradiating the soft X-ray emission region in each case, the table suggests a trend with a major fraction of the ionized outflow being hidden from our view in type 2 objects. This is an expanded and revised version of table 1 in Pounds et al. (2005).

Galaxy	Optical type	L_{2-10} (erg s ⁻¹)	L_{SX} (erg s ⁻¹)	Ratio (L_{SX}/L_{2-10})	L_{SX} (erg s ⁻¹)	Ratio (L_{SX}/L_{2-10})
NGC 4051	Seyfert 1	3.5×10^{41}	3.5×10^{40}	10 per cent	3.5×10^{40}	10 per cent
1H 0419-577	QSO 1	2.5×10^{44}	3×10^{43}	12 per cent	3.2×10^{43}	13 per cent
2M 2344+1221	QSO 1	5.2×10^{43}	6.1×10^{42}	11 per cent	10.1×10^{42}	19 per cent
Mkn 3	Seyfert 2	1.5×10^{43}	1.6×10^{41}	1.1 per cent	2.4×10^{41}	1.6 per cent
NGC 1068	Seyfert 2	2.3×10^{43}	1.5×10^{41}	0.6 per cent	1.7×10^{41}	0.7 per cent
2M 0918+2117	QSO 1.5	8.6×10^{43}	2.7×10^{42}	3.1 per cent	3.8×10^{42}	4.4 per cent

Fe xxv the measured line energy would imply an outflow velocity of $v \sim 0.15c$.

The broader absorption feature near ~ 7.6 keV (~ 8.7 keV in the AGN rest frame), only detected in the pn camera, is better modelled with an absorption edge. Intriguingly, the K edge of He-like Fe xxv (threshold energy 8.83 keV; Verner et al. 1996) lies close to the derived edge energy. With that identification and a threshold cross section of 2×10^{-20} cm² (Verner et al. 1996), the measured edge optical depth of ~ 0.3 implies an absorbing column density of $N_{\text{Fe xxv}} \sim 1.5 \times 10^{19}$ cm⁻². Assuming Fe xxv to be the dominant ion (likely over a rather wide range of ionization parameter in a highly ionized gas, and noting no evidence for an Fe xxvi edge), this corresponds, for a solar abundance of Fe, to a column density of $N_{\text{H}} \sim 5 \times 10^{23}$ cm⁻².

There have been an increasing number of reports of highly ionized gas imprinting Fe K features on AGN X-ray spectra. Due to the relatively low cross-sections at those energies, the derived column densities are always high. One of the first (Hasinger, Schartel & Komossa 2002) suggested an interpretation of features in the high-redshift broad absorption line (BAL) quasar APM08279+5255 as Fe xv–Fe xvi edge absorption in a column density of $N_{\text{H}} \sim 10^{23}$ cm⁻². More often, higher quality spectra have shown absorption lines of Fe xxv or Fe xxvi, in some cases also indicating rapidly outflowing gas (Pounds et al. 2003; Reeves, O’Brien & Ward 2003; Young et al. 2005; Pounds & Page 2006).

But are the absorption features seen in the present spectra of 2MASS 0918+2117 real? Visual examination of the respective background spectra shows the background rate rising strongly above ~ 6 keV in the MOS and ~ 7 keV in the pn data. While the pn camera background is also enhanced near ~ 8 keV (probably due to the Cu K line arising from the electronics board, Strüder et al. 2001), the ‘absorption edge’ observed at ~ 7.6 keV is statistically significant in the source-only data.

In conclusion, while continuing to regard the absorption features in the Fe K band as doubtful, we believe they are of sufficient potential interest to retain for future checking with better data.

6 SUMMARY

(i) Analysis of a new *XMM-Newton* observation of the type 1.5 QSO 2MASS 0918+2117 confirms the presence of a cold absorbing column consistent with the red optical nucleus and intermediate optical type.

(ii) Comparison with the previous *XMM-Newton* observation when 2MASS 0918+2117 was in a much lower flux state, provides further evidence that strong variability in AGN X-ray spectra arises

when a relatively steep ($\Gamma \gtrsim 2$) power-law continuum overcomes a more complex and quasi-constant underlying spectrum. Previous explanations of hard low-state spectra ($\gtrsim 2$ keV) being reflection dominated appear also to apply to 2MASS 0918+2117.

(iii) Spectral structure seen below ~ 1 keV in the 2003 *XMM-Newton* observation of 2MASS 0918+2117 and interpreted as emission from ionized gas, appears again to be present in the 2005 observation.

(iv) Comparison of the relative strength of the soft X-ray emission in a number of type 1 and type 2 AGN shows the former to be typically an order of magnitude greater, suggesting ionized outflows originate well within the BLR, and so are substantially obscured in type 2 sources. The intermediate value found here for 2MASS 0918+2117 may then be consistent with its intermediate optical type.

(v) Evidence for strong absorption in the higher energy channels of both EPIC cameras is reduced but is still statistically significant when background features are removed. If real, the high energy absorption implies a large column of highly ionized gas in the line of sight to 2MASS 0918+2117.

ACKNOWLEDGMENTS

The results reported here are based on the observations obtained with *XMM-Newton*, an ESA science mission with instruments and contributions directly funded by ESA Member States and the USA (NASA). The authors wish to thank the SOC and the SSC teams for organizing the *XMM-Newton* observations and initial data reduction. BJW is grateful for the financial support of *XMM-Newton* GO grant: NNG04GD27G.

REFERENCES

- Arnaud K. A., 1996, in Jacoby G. H., Barnes J., eds, ASP Conf. Ser. Vol. 101, Astronomical Data and Software Systems V. Astron. Soc. Pac., San Francisco, p. 17
- Barkhouse W. A., Hall P. B., 2001, AJ, 121, 2843
- Cutri R. et al., 2001, in Clowes R., Adamson A., Bromage G., eds, ASP Conf. Ser. Vol. 32, New Era of Wide Field Astronomy. Astron. Soc. Pac., San Francisco, p. 78
- Cutri R. et al., 2003, On-line Catalogue II/246, IPAC/Cal Tech
- Fabian A. C., Vaughan S., 2003, MNRAS, 340, L28
- Haardt F., Maraschi L., Ghisellini G., 1997, ApJ, 476, 620
- Hasinger G., Schartel N., Komossa S., 2002, ApJ, 573, L77
- Marconi A., Risaliti G., Gilli R., Hunt L. K., Maiolino R., Salvati M., 2004, MNRAS, 351, 169
- Nandra K., Pounds K. A., 1994, MNRAS, 268, 405
- Pounds K. A., Page K. L., 2006, MNRAS, 372, 1275

- Pounds K. A., Reeves J. N., King A. R., Page K. L., O'Brien P. T., Turner M. J. L., 2003, *MNRAS*, 345, 705
- Pounds K. A., Reeves J. N., Page K. L., O'Brien P. T., 2004, *ApJ*, 616, 696
- Pounds K. A., Wilkes B. J., Page K. L., 2005, *MNRAS*, 362, 784
- Reeves J. N., O'Brien P. T., Ward M. J., 2003, *ApJ*, 593, L65
- Smith P. S., Schmidt G. D., Hines D. C., Cutri R. M., Nelson B. O., 2002, *ApJ*, 569, 23
- Smith P. S., Schmidt G. D., Hines D. C., Foltz C. B., 2003, *ApJ*, 593, 676
- Strüder L. et al., 2001, *A&A*, 365, L18
- Turner M. J. L. et al., 2001, *A&A*, 365, L27
- Verner D. A., Ferland G. J., Korista K. T., Yakovlev D. G., 1996, *ApJ*, 465, 487
- Wilkes B. J., Schmidt G. D., Cutri R. M., Ghosh H., Hines D. C., Nelson B., Smith P. S., 2002, *ApJ*, 564, L65
- Wilkes B. J., Pounds K. A., Schmidt G. D., Smith P. S., Cutri R. M., Ghosh H., Nelson B., Hines D. C., 2005, *ApJ*, 634, 183 (W05)
- Young A. J., Lee J. C., Fabian A. C., Reynolds C. S., Gibson R. R., Canizares C. R., 2005, *ApJ*, 631, 733

This paper has been typeset from a $\mathrm{T}_{\mathrm{E}}\mathrm{X}/\mathrm{L}^{\mathrm{A}}\mathrm{T}_{\mathrm{E}}\mathrm{X}$ file prepared by the author.